and so addresses a crucial problem in structural biology. This is done by the remarkably successful method of single-particle image reconstruction, in which images of the same protein, lying in random orientations within a thin film of vitreous ice, are combined in the correct orientation to form a three-dimensional reconstructed charge-density map at nanometre or better resolution. The summation over many particles achieves the same radiation-damage-reduction effect as does crystallographic redundancy in protein crystallography. Finally, Section 2.5.8 describes experience with the application of numerical direct methods to the phase problem in electron diffraction. Although direct imaging 'solves' the phase problem, there are many practical problems in combining electron-microdiffraction intensities with corresponding high-resolution images of a structure over a large tilt range. In cases where multiple scattering can be minimized, some success has therefore been obtained using direct phasing methods, as reviewed in this section.

For most inorganic materials the complications of many-beam dynamical diffraction processes prevent the direct application of these techniques of image analysis, which depend on having a linear relationship between the image intensity and the value of the projected potential distribution of the sample. The smaller sensitivities to radiation damage can, to some extent, remove the need for the application of such methods by allowing direct visualization of structure with ultra-high-resolution images and the use of microdiffraction techniques.

2.5.2. Electron diffraction and electron microscopy[1]

By J. M. Cowley

2.5.2.1. Introduction

The contributions of electron scattering to the study of the structures of crystalline solids are many and diverse. This section will deal only with the scattering of high-energy electrons (in the energy range of 10^4 to 10^6 eV) in transmission through thin samples of crystalline solids and the derivation of information on crystal structures from diffraction patterns and high-resolution images. The range of wavelengths considered is from about 0.122 Å (12.2 pm) for 10 kV electrons to 0.0087 Å (0.87 pm) for 1 MeV electrons. Given that the scattering amplitudes of atoms for electrons have much the same form and variation with $(\sin\theta)/\lambda$ as for X-rays, it is apparent that the angular range for strong scattering of electrons will be of the order of 10^{-2} rad. Only under special circumstances, usually involving multiple elastic and inelastic scattering from very thick specimens, are scattering angles of more than 10^{-1} rad of importance.

The strength of the interaction of electrons with matter is greater than that of X-rays by two or three orders of magnitude. The single-scattering, first Born approximation fails significantly for scattering from single heavy atoms. Diffracted beams from single crystals may attain intensities comparable with that of the incident beam for crystal thicknesses of 10^2 Å, rather than 10^4 Å or more. It follows that electrons may be used for the study of very thin samples, and that dynamical scattering effects, or the coherent interaction of multiply scattered electron waves, will modify the diffracted amplitudes in a significant way for all but very thin specimens containing only light atoms.

The experimental techniques for electron scattering are largely determined by the possibility of focusing electron beams by use of strong axial magnetic fields, which act as electron lenses having focal lengths as short as 1 mm or less. Electron microscopes employing such lenses have been produced with resolutions approaching 1 Å. With such instruments, images showing individual isolated atoms of moderately high atomic number may be obtained. The resolution available is sufficient to distinguish neighbouring rows of adjacent atoms in the projected structures of thin crystals viewed in favourable orientations. It is therefore possible in many cases to obtain information on the structure of crystals and of crystal defects by direct inspection of electron micrographs.

The electromagnetic electron lenses may also be used to form electron beams of very small diameter and very high intensity. In particular, by the use of cold field-emission electron guns, it is possible to obtain a current of 10^{-10} A in an electron beam of diameter 10 Å or less with a beam divergence of less than 10^{-2} rad, *i.e.* a current density of 10^4 A cm^{-2} or more. The magnitudes of the electron scattering amplitudes then imply that detectable signals may be obtained in diffraction from assemblies of fewer than 10^2 atoms. On the other hand, electron beams may readily be collimated to better than 10^{-6} rad.

The cross sections for inelastic scattering processes are, in general, less than for the elastic scattering of electrons, but signals may be obtained by the observation of electron energy losses, or the production of secondary radiations, which allow the analysis of chemical compositions or electronic excited states for regions of the crystal 100 Å or less in diameter.

On the other hand, the transfer to the sample of large amounts of energy through inelastic scattering processes produces radiation damage which may severely limit the applicability of the imaging and diffraction techniques, especially for biological and organic materials, unless the information is gathered from large specimen volumes with low incident electron beam densities.

Structure analysis of crystals can be performed using electron diffraction in the same way as with X-ray or neutron diffraction. The mathematical expressions and the procedures are much the same. However, there are peculiarities of the electron-diffraction case which should be noted.

(1) Structure analysis based on electron diffraction is possible for thin specimens for which the conditions for kinematical scattering are approached, *e.g.* for thin mosaic single-crystal specimens, for thin polycrystalline films having a preferred orientation of very small crystallites or for very extensive, very thin single crystals of biological molecules such as membranes one or a few molecules thick.

(2) Dynamical diffraction effects are used explicitly in the determination of crystal symmetry (with no Friedel's law limitations) and for the measurement of structure amplitudes with high accuracy.

(3) For many radiation-resistant materials, the structures of crystals and of some molecules may be determined directly by imaging atom positions in projections of the crystal with a resolution of 2 Å or better. The information on atom positions is not dependent on the periodicity of the crystal and so it is equally possible to determine the structures of individual crystal defects in favourable cases.

(4) Techniques of microanalysis may be applied to the determination of the chemical composition of regions of diameter 100 Å or less using the same instrument as for diffraction, so that the chemical information may be correlated directly with morphological and structural information.

(5) Crystal-structure information may be derived from regions containing as few as 10^2 or 10^3 atoms, including very small crystals and single or multiple layers of atoms on surfaces.

The material of this section is also reviewed in the text by Spence (2003).

2.5.2.2. The interactions of electrons with matter

(1) The *elastic* scattering of electrons results from the interaction of the charged electrons with the electrostatic potential distribution, $\varphi(\mathbf{r})$, of the atoms or crystals. An incident electron of kinetic energy eW gains energy $e\varphi(\mathbf{r})$ in the potential field. Alternatively it may be stated that an incident electron wave of

[1] Questions related to this section may be addressed to Professor J. C. H. Spence (see list of contributing authors).

wavelength $\lambda = h/mv$ is diffracted by a region of variable refractive index

$$n(\mathbf{r}) = k/K_0 = \{[W + \varphi(\mathbf{r})]/W\}^{1/2} \simeq 1 + \varphi(\mathbf{r})/2W.$$

(2) The most important *inelastic* scattering processes are:

(*a*) thermal diffuse scattering, with energy losses of the order of 2×10^{-2} eV, separable from the elastic scattering only with specially devised equipment; the angular distribution of thermal diffuse scattering shows variations with $(\sin\theta)/\lambda$ which are much the same as for the X-ray case in the kinematical limit;

(*b*) bulk plasmon excitation, or the excitation of collective energy states of the conduction electrons, giving energy losses of 3 to 30 eV and an angular range of scattering of 10^{-4} to 10^{-3} rad;

(*c*) surface plasmons, or the excitation of collective energy states of the conduction electrons at discontinuities of the structure, with energy losses less than those for bulk plasmons and a similar angular range of scattering;

(*d*) interband or intraband excitation of valence-shell electrons giving energy losses in the range of 1 to 10^2 eV and an angular range of scattering of 10^{-4} to 10^{-2} rad;

(*e*) inner-shell excitations, with energy losses of 10^2 eV or more and an angular range of scattering of 10^{-3} to 10^{-2} rad, depending on the energy losses involved.

(3) In the original treatment by Bethe (1928) of the elastic scattering of electrons by crystals, the Schrödinger equation is written for electrons in the periodic potential of the crystal; *i.e.*

$$\nabla^2\psi(\mathbf{r}) + K_0^2[1 + \varphi(\mathbf{r})/W]\psi(\mathbf{r}) = 0, \tag{2.5.2.1}$$

where

$$\begin{aligned}\varphi(\mathbf{r}) &= \int V(\mathbf{u}) \exp\{-2\pi i\mathbf{u}\cdot\mathbf{r}\}\,\mathrm{d}\mathbf{u} \\ &= \sum_{\mathbf{h}} V_{\mathbf{h}} \exp\{-2\pi i\mathbf{h}\cdot\mathbf{r}\},\end{aligned} \tag{2.5.2.2}$$

$\mathbf{K}_0$ is the wavevector in zero potential (outside the crystal) (magnitude $2\pi/\lambda$) and W is the accelerating voltage. The solutions of the equation are Bloch waves of the form

$$\psi(\mathbf{r}) = \sum_{\mathbf{h}} C_{\mathbf{h}}(\mathbf{k}) \exp\{-i(\mathbf{k}_0 + 2\pi\mathbf{h})\cdot\mathbf{r}\}, \tag{2.5.2.3}$$

where $\mathbf{k}_0$ is the incident wavevector in the crystal and $\mathbf{h}$ is a reciprocal-lattice vector. Substitution of (2.5.2.2) and (2.5.2.3) in (2.5.2.1) gives the dispersion equations

$$(\kappa^2 - k_{\mathbf{h}}^2)C_{\mathbf{h}} + \sum_{\mathbf{g}}{}' V_{\mathbf{h}-\mathbf{g}}C_{\mathbf{g}} = 0. \tag{2.5.2.4}$$

Here κ is the magnitude of the wavevector in a medium of constant potential V_0 (the 'inner potential' of the crystal). The refractive index of the electron in the average crystal potential is then

$$n = \kappa/K = (1 + V_0/W)^{1/2} \simeq 1 + V_0/2W. \tag{2.5.2.5}$$

Since V_0 is positive and of the order of 10 V and W is 10^4 to 10^6 V, $n - 1$ is positive and of the order of 10^{-4}.

Solution of equation (2.5.2.4) gives the Fourier coefficients $C_{\mathbf{h}}^{(i)}$ of the Bloch waves $\psi^{(i)}(\mathbf{r})$ and application of the boundary conditions gives the amplitudes of individual Bloch waves (see Chapter 5.2).

(4) The experimentally important case of transmission of high-energy electrons through thin specimens is treated on the assumption of a plane wave incident in a direction almost perpendicular to an infinitely extended plane-parallel lamellar crystal, making use of the *small-angle scattering approximation* in which the forward-scattered wave is represented in the paraboloidal approximation to the sphere. The incident-beam direction, assumed to be almost parallel to the z axis, is unique and the z component of $\mathbf{k}$ is factored out to give

$$\nabla^2\psi + 2k\sigma\varphi\psi = \pm i2k\frac{\partial\psi}{\partial z}, \tag{2.5.2.6}$$

where $k = 2\pi/\lambda$ and $\sigma = 2\pi me\lambda/h^2$. [See Lynch & Moodie (1972), Portier & Gratias (1981), Tournarie (1962), and Chapter 5.2.]

This equation is analogous to the time-dependent Schrödinger equation with z replacing t. Retention of the $\pm$ signs on the right-hand side is consistent with both ψ and ψ^* being solutions, corresponding to propagation in opposite directions with respect to the z axis. The double-valued solution is of importance in consideration of reciprocity relationships which provide the basis for the description of some dynamical diffraction symmetries. (See Section 2.5.3.)

(5) The integral form of the wave equation, commonly used for scattering problems, is written, for electron scattering, as

$$\psi(\mathbf{r}) = \psi^{(0)}(\mathbf{r}) + (\sigma/\lambda)\int \frac{\exp\{-i\mathbf{k}|\mathbf{r} - \mathbf{r}'|\}}{|\mathbf{r} - \mathbf{r}'|}\varphi(\mathbf{r}')\psi(\mathbf{r}')\,\mathrm{d}\mathbf{r}'. \tag{2.5.2.7}$$

The wavefunction $\psi(\mathbf{r})$ within the integral is approximated by using successive terms of a Born series

$$\psi(\mathbf{r}) = \psi^{(0)}(\mathbf{r}) + \psi^{(1)}(\mathbf{r}) + \psi^{(2)}(\mathbf{r}) + \ldots. \tag{2.5.2.8}$$

The first Born approximation is obtained by putting $\psi(\mathbf{r}) = \psi^{(0)}(\mathbf{r})$ in the integral and subsequent terms $\psi^{(n)}(\mathbf{r})$ are generated by putting $\psi^{(n-1)}(\mathbf{r})$ in the integral.

For an incident plane wave, $\psi^{(0)}(\mathbf{r}) = \exp\{-i\mathbf{k}_0\cdot\mathbf{r}\}$ and for a point of observation at a large distance $\mathbf{R} = \mathbf{r} - \mathbf{r}'$ from the scattering object ($|\mathbf{R}| \gg |\mathbf{r}'|$), the first Born approximation is generated as

$$\psi^{(1)}(\mathbf{r}) = \frac{i\sigma}{\lambda R}\exp\{-i\mathbf{k}\cdot\mathbf{R}\}\int \varphi(\mathbf{r}')\exp\{i\mathbf{q}\cdot\mathbf{r}'\}\,\mathrm{d}\mathbf{r}',$$

where $\mathbf{q} = \mathbf{k} - \mathbf{k}_0$ or, putting $\mathbf{u} = \mathbf{q}/2\pi$ and collecting the pre-integral terms into a parameter μ,

$$\Psi(\mathbf{u}) = \mu\int \varphi(\mathbf{r})\exp\{2\pi i\mathbf{u}\cdot\mathbf{r}\}\,\mathrm{d}\mathbf{r}. \tag{2.5.2.9}$$

This is the Fourier-transform expression which is the basis for the *kinematical scattering approximation*. It is derived on the basis that all $\psi^{(n)}(\mathbf{r})$ terms for $n \neq 0$ are very much smaller than $\psi^{(0)}(\mathbf{r})$ and so is a weak scattering approximation.

In this approximation, the scattered amplitude for an atom is related to the atomic structure amplitude, $f(\mathbf{u})$, by the relationship, derived from (2.5.2.8),

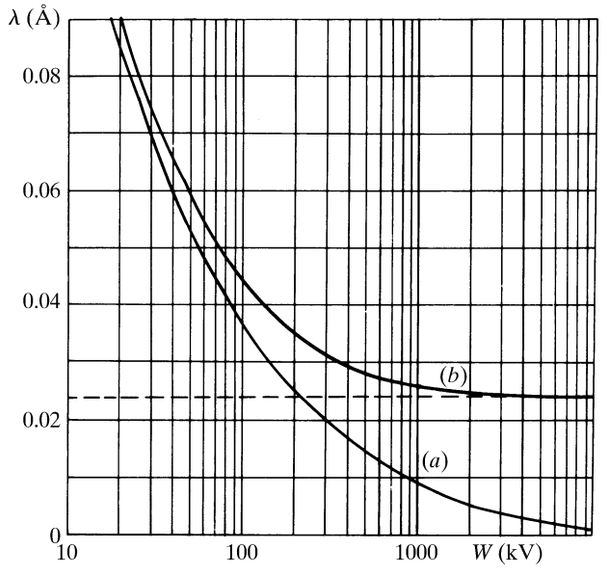

Fig. 2.5.2.1. The variation with accelerating voltage of electrons of (*a*) the wavelength, λ and (*b*) the quantity $\lambda[1 + (h^2/m_0^2c^2\lambda^2)] = \lambda_c/\beta$ which is proportional to the interaction constant σ [equation (2.5.2.14)]. The limit is the Compton wavelength λ_c (after Fujiwara, 1961).

$$\psi(\mathbf{r}) = \exp\{-i\mathbf{k}_0 \cdot \mathbf{r}\} + i\frac{\exp\{-i\mathbf{k} \cdot \mathbf{r}\}}{R\lambda}\sigma f(\mathbf{u}),$$
$$f(\mathbf{u}) = \int \varphi(\mathbf{r}) \exp\{2\pi i\mathbf{u} \cdot \mathbf{r}\}\, \mathrm{d}\mathbf{r}. \qquad (2.5.2.10)$$

For centrosymmetrical atom potential distributions, the $f(\mathbf{u})$ are real, positive and monotonically decreasing with $|\mathbf{u}|$. A measure of the extent of the validity of the first Born approximation is given by the fact that the effect of adding the higher-order terms of the Born series may be represented by replacing $f(\mathbf{u})$ in (2.5.2.10) by the complex quantities $f(\mathbf{u}) = |\mathbf{f}| \exp\{i\eta(\mathbf{u})\}$ and for single heavy atoms the phase factor η may vary from 0.2 for $|\mathbf{u}| = 0$ to 4 or 5 for large $|\mathbf{u}|$, as seen from the tables of *IT* C (2004, Section 4.3.3).

(6) Relativistic effects produce appreciable variations of the parameters used above for the range of electron energies considered. The relativistic values are

$$m = m_0(1 - v^2/c^2)^{-1/2} = m_0(1 - \beta^2)^{-1/2}, \qquad (2.5.2.11)$$
$$\lambda = h[2m_0|e|W(1 + |e|W/2m_0c^2)]^{-1/2} \qquad (2.5.2.12)$$
$$= \lambda_c(1 - \beta^2)^{1/2}/\beta, \qquad (2.5.2.13)$$

where λ_c is the Compton wavelength, $\lambda_c = h/m_0c = 0.0242$ Å, and

$$\sigma = 2\pi me\lambda/h^2 = (2\pi m_0 e/h^2)(\lambda_c/\beta)$$
$$= 2\pi/\{\lambda W[1 + (1 - \beta^2)^{1/2}]\}. \qquad (2.5.2.14)$$

Values for these quantities are listed in *IT* C (2004, Section 4.3.2). The variations of λ and σ with accelerating voltage are illustrated in Fig. 2.5.2.1. For high voltages, σ tends to a constant value, $2\pi m_0 e\lambda_c/h^2 = e/\hbar c$.

2.5.2.3. Recommended sign conventions

There are two alternative sets of signs for the functions describing wave optics. Both sets have been widely used in the literature. There is, however, a requirement for internal consistency within a particular analysis, independently of which set is adopted. Unfortunately, this requirement has not always been met and, in fact, it is only too easy at the outset of an analysis to make errors in this way. This problem might have come into prominence somewhat earlier were it not for the fact that, for centrosymmetric crystals (or indeed for centrosymmetric projections in the case of planar diffraction), only the signs used in the transmission and propagation functions can affect the results. It is not until the origin is set away from a centre of symmetry that there is a need to be consistent in every sign used.

Signs for electron diffraction have been chosen from two points of view: (1) defining as positive the sign of the exponent in the structure-factor expression and (2) defining the forward propagating free-space wavefunction with a positive exponent.

The second of these alternatives is the one which has been adopted in most solid-state and quantum-mechanical texts.

The first, or *standard crystallographic* convention, is the one which could most easily be adopted by crystallographers accustomed to retaining a positive exponent in the structure-factor equation. This also represents a consistent *International Tables* usage. It is, however, realized that both conventions will continue to be used in crystallographic computations, and that there are by now a large number of operational programs in use.

It is therefore recommended (*a*) that a particular sign usage be indicated as either *standard crystallographic* or *alternative crystallographic* to accord with Table 2.5.2.1, whenever there is a need for this to be explicit in publication, and (*b*) that either one or other of these systems be adhered to throughout an analysis in a self-consistent way, even in those cases where, as indicated above, some of the signs appear to have no effect on one particular conclusion.

2.5.2.4. Scattering of electrons by crystals; approximations

The forward-scattering approximation to the many-beam dynamical diffraction theory outlined in Chapter 5.2 provides the basis for the calculation of diffraction intensities and electron-microscope image contrast for thin crystals. [See Cowley (1995), Chapter 5.2 and *IT* C (2004) Sections 4.3.6 and 4.3.8.] On the other hand, there are various approximations which provide relatively simple analytical expressions, are useful for the determination of diffraction geometry, and allow estimates to be made of the relative intensities in diffraction patterns and electron micrographs in favourable cases.

(*a*) *The kinematical approximation*, derived in Section 2.5.2.2 from the first Born approximation, is analagous to the corresponding approximation of X-ray diffraction. It assumes that the scattering amplitudes are directly proportional to the three-dimensional Fourier transform of the potential distribution, $\varphi(\mathbf{r})$.

$$V(\mathbf{u}) = \int \varphi(\mathbf{r}) \exp\{2\pi i\mathbf{u} \cdot \mathbf{r}\}\, \mathrm{d}\mathbf{r}, \qquad (2.5.2.15)$$

so that the potential distribution $\varphi(\mathbf{r})$ takes the place of the charge-density distribution, $\rho(\mathbf{r})$, relevant for X-ray scattering.

The validity of the kinematical approximation as a basis for structure analysis is severely limited. For light-atom materials, such as organic compounds, it has been shown by Jap & Glaeser (1980) that the thickness for which the approximation gives reasonable accuracy for zone-axis patterns from single crystals is of the order of 100 Å for 100 keV electrons and increases, approximately as σ^{-1}, for higher energies. The thickness limits quoted for polycrystalline samples, having crystallite dimensions smaller than the sample thickness, are usually greater (Vainshtein, 1956). For heavy-atom materials the approximation is more limited since it may fail significantly for single heavy atoms.

(*b*) *The phase-object approximation* (POA), or high-voltage limit, is derived from the general many-beam dynamical